SABA Publishing

Journal of Mathematical Analysis and Modeling
jmam.sabapub.com
ISSN 2709-5924

J Math Anal & Model
(2023)4(2) : 121-145
doi:10.48185/jmam.v4i2.942

Mathematical Analysis of COVID-19 model with Vaccination and Partial Immunity to Reinfection

FRANCIS MUSILI MULI [a,*], BENARD OKELO [b], RICHARD MAGWANGA [c], OMOLO ONGATI [d]

[a,b,d] Department of Pure and Applied Mathematics, Jaramogi Oginga Odinga University of Science and Technology (JOOUST)

[c] Department of Biological Sciences, Jaramogi Oginga Odinga University of Science and Technology (JOOUST)

• *Received: 20 December 2023* • *Accepted: 28 December 2023* • *Published Online: 30 December 2023*

Abstract

COVID-19 is an infectious respiratory disease caused by a new virus, called SARS-CoV-2. Since its inception, it has been a major cause of deaths and illnesses in the general population across the globe. In this paper, we have formulated and theoretically analyzed a non-linear deterministic model for COVID-19 transmission dynamics by incorporating vaccination of the susceptible population. The system properties, such as the boundedness of solutions, the basic reproduction number R_0, the local stability of disease-free equilibrium(DFE), and endemic equilibrium (EE) points, are explored. Besides, the Lyapunov function is utilized to prove the global stability of both DFE and EE. The bifurcation analysis was carried out by utilizing the center manifold theory. Then, the model is fitted with real COVID-19 cumulative data of infected cases in Kenya as from March 30, 2020, to March 30, 2022. Furthermore, sensitivity analysis was performed for the proposed model to ascertain the relative significance of model parameters to COVID-19 transmission dynamics. The simulations revealed that the spread of COVID-19 can be curtailed not only via vaccination of susceptible populations but also increased administration of COVID-19 booster vaccine to the vaccinated persons and early detection and treatment of asymptomatic individuals.

Keywords: COVID-19, Vaccine, Stability analysis, Reinfection, Parameter estimation.

1. Introduction

It is uncontested that COVID-19 has caused unprecedented pain and deaths around the globe. COVID-19 is an infectious disease that emerged in Wuhan in China in December 2019 and spread rapidly around that country and ultimately pervaded other countries.

Among the East African countries, the index case was first identified in Kenya on 13th March 2020, which was imported by a Kenyan who had arrived from the USA [1]. Surveillance was enhanced at all official border points of entry and exit to contain and prevent

*Francis Musili Muli: framuli2011@gmail.com

further infections. Due to its novelty, concerted efforts from health professionals and mathematicians have been instituted to evaluate scenarios that greatly minimize infections. For instance, a mathematical model highlighting the dynamics of COVID-19 transmission impacts and preventive measures was developed by [2]. This study formulated a Susceptible-Masked-Unmasked-Exposed-Infected-Hospitalized-Recovered model type involving the human population. The sensitivity analysis underscored the importance of wearing masks, especially in crowded populations as well as when attending to isolated COVID-19 patients.

A five compartmental COVID-19 model of SEIQR type was formulated and analyzed by [3]. The model sought to identify the factors that immensely contribute to disease dissemination and persistence in the population. The findings of this study revealed that the most sensitive parameter is the contact rate among susceptible and infectious individuals, followed by the recovery rate of infectious individuals. The study by [4] investigated the optimal control strategies of COVID-19 dynamics. The study findings suggested that the simultaneous administration of vaccines to the susceptible population and increasing the rate of treatment of the infectives is the best approach for abasing COVID-19 transmissions. A study on fractional Order modeling of predicting COVID-19 with isolation and vaccination strategies in Morocco was conducted by [5]. This study underscored the importance of adherence to COVID-19 preventive measures, vaccination, and adaptation if this pandemic is to be weeded out from the community.

A COVID-19 transmission model encompassing symptomatic and asymptomatic states was formulated and analyzed by [6]. This research established that the most sensitive parameters about reproduction R_0 are the transmission coefficient and the movement rate of individuals from the exposed class to the symptomatically infected class. The study's finding suggested that it should be of particular interest to all that in the fight against the COVID-19 pandemic, the exposure as a result of contact with infected individuals, especially those who are asymptomatic, should be curtailed. Moreover, the study on analysis of the mitigation strategies for COVID-19 was carried out by [7]. The results from the study unveiled that in a scenario where the recovered individuals do not develop permanent immunity to reinfection, backward bifurcation at $R_0 < 1$ occurs. This immensely complicates the government and health professionals' efforts in the war against the disease. The study further disclosed that backward bifurcation is precluded in the absence of reinfection, and instead, forward bifurcation sets in. This implies that the DFE is globally asymptotically stable for $R_0 < 1$. Reinfection by the family of coronaviruses is possible, as it is indicated in [8] and [9].

Although the duration it takes for a recovered individual to lose natural immunity is still obscure, we cannot disregard its influence as far as COVID-19 transmission dynamics is concerned. Motivated by the study by [10], we formulated and analyzed a $S_hV_hE_hI_{hA}I_hR_h$ which unlike the model above we have included a vaccinated class that can go back to susceptible population due to waning of vaccine-induced immunity and assumed that a fraction of the recovered individuals become susceptible due to waning of the natural immunity. To our knowledge, such considerations have not been factored in the existing COVID-19 models.

This paper is organized as follows: In section 1, the model formulation is described. A comprehensive mathematical analysis encompassing model's positivity and boundedness,

stability and bifurcation analysis are presented in section 2. Section 3 is devoted to curve fitting, parameter estimation and sensitivity analysis. Numerical simulations are presented in section 4. Finally, our discussion and conclusions are presented in section 5.

2. Model formulation

In this section, we formulate a model of the form $S_h V_h E_h I_{hA} I_h R_h$ to analyze COVID-19 transmission dynamics. In this study, the whole population $N_h(t)$ is stratified into six (6) mutually exclusive compartments, S_h, V_h, E_h, I_{hA}, I_h and R_h which respectively represent the susceptible, vaccinated, exposed, asymptomatic, symptomatic and Recovered individuals.

Equation of the model are derived as follows: The susceptible population's growth is due to immigration or birth at a rate π [11] as well as the reinfection of recovered individuals at the rate τ. COVID-19 vaccine is administered to the susceptible population at the rate θ. This vaccine-induced immunity is assumed to wane at the rate φ. Furthermore, the susceptible individuals progress to the exposed phase upon interaction with the asymptomatic and the symptomatic individuals. The force of infection λ is thus expressed as:

$$\lambda = \beta(\xi I_{hA} + I_h)$$

where parameter β is the transmission coefficient which accounts for contacts capable of leading to infection, while $\xi \in (0,1)$ is the modification parameter which accounts for presumed reduction in infectiousness of the asymptomatic individuals relative to the symptomatic individuals. All the population clusters are presumed to decrease at a constant value μ which accounts for natural death rate. The rate of progression of both susceptible and vaccinated individuals is thus given as:

$$\frac{dS_h}{dt} = \pi + \varphi V_h + \tau R_h - (\lambda + \mu + \theta) S_h$$
$$\frac{dV_h}{dt} = \theta S_h - (\mu + \varphi) V_h$$

The growth of the exposed population is necessitated by the susceptible at the rate λ and it is diminished at a constant rate ω when a fraction ϵ of the individuals develop symptoms and the rest $(1-\epsilon)$ progress to asymptomatic compartment. It is worth noting that the exposed individuals are those who are infected with COVID-19, do not manifest symptoms of the disease yet and they register negative when subjected to polymerase chain reaction (PCR) tests. Patients are said to be in latency phase and are regarded as non-infectious. COVID-19 is known to have an incubation period whose range is from 2 to 14 days between exposure and development of symptoms [10]. Thus we obtain the expression;

$$\frac{dE_h}{dt} = \lambda S_h - (\mu + \omega) E_h$$

The asymptomatic class class I_{hA} consist of those who do not develop clinical COVID-19 symptoms after the disease incubation. In this study we assume that the asymptomatic individuals become sick of COVID-19 if left untreated since any infection compromises

one's innate immune system rendering one vulnerable to infection from other COVID-19 variants or can recover from the disease. These silent COVID-19 spreaders recover at the rate κ. In fact κ is the measure of efficacy of identification and treatment of the asymptomatic individuals. The expression for asymptomatic population thus becomes:

$$\frac{dI_{hA}}{dt} = (1-\epsilon)\omega E_h - (\mu+\alpha)I_{hA}$$

Besides the natural death rate μ, the symptomatic individuals are diminished by the COVID-19-induced death rate at δ. The parameter γ accounts for the successful treatment and recovery rate of the symptomatic. The expressions for symptomatic is thus given as:

$$\frac{dI_h}{dt} = \epsilon\omega E_h + (1-\kappa)\alpha I_{hA} - (\mu+\gamma+\delta)I_h$$

Finally, the growth of the recovered individuals is generated by the recovery of the asymptomatic and symptomatic and is diminished due to the waning of natural immunity at the rate τ. We express the rate of recovery equation as:

$$\frac{dR_h}{dt} = \gamma I_h + \alpha\kappa I_{hA} - (\mu+\tau)R_h$$

Thus, it follows that our model consists of the following system of non-linear differential equations:

$$\begin{aligned}
\frac{dS_h}{dt} &= \pi + \tau R_h + \varphi V_n - (\lambda+\mu+\theta)S_h \\
\frac{dV_h}{dt} &= \theta S_h - (\varphi+\mu)V_h \\
\frac{dE_h}{dt} &= \lambda S_h - (\omega+\mu)E_h \\
\frac{dI_{hA}}{dt} &= \omega(1-\epsilon)E_h - (\mu+\alpha)I_{hA} \\
\frac{dI_h}{dt} &= \omega\epsilon E_h + (1-\kappa)\alpha I_{hA} - (\mu+\delta+\gamma)I_h \\
\frac{dR_h}{dt} &= \kappa\alpha I_{hA} + \gamma I_h - (\mu+\tau)R_h
\end{aligned} \tag{2.1}$$

Table 1: Definition of state variables

Variable	Definition
S_h	Human population susceptible to COVID-19 disease
V_h	Fully vaccinated population
E_h	Individuals in a latency period
I_{hA}	Asymptomatic persons
I_h	Symptomatic persons
R_h	Recovered population.

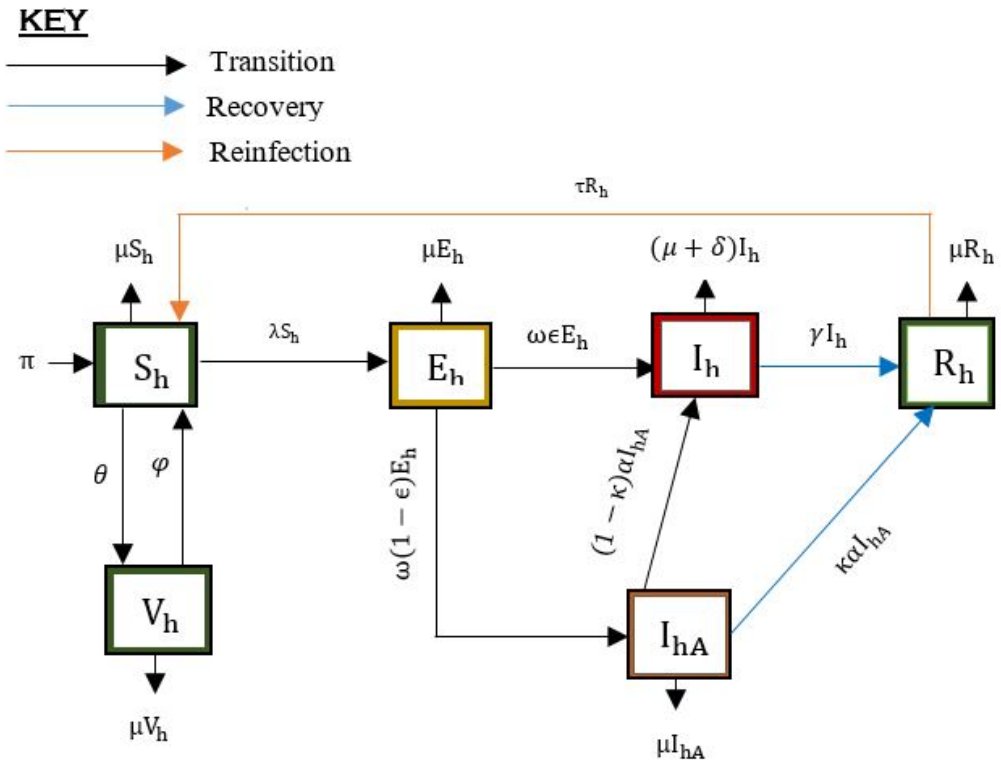

Figure 1: General COVID-19 flow diagram for COVID-19 model 1

2.1. Model analysis

This section discusses the proposed model's basic properties, including the solution's positivity, the feasible region, model's equilibrium points, and the stability of the equilibrium points.

Theorem 2.1. *If* $S_h(0) \geqslant 0, V_h(0) \geqslant 0, E_h(0) \geqslant 0, I_{hA}(0) \geqslant 0, I_h(0) \geqslant 0$ *and* $R_h(0) \geqslant 0$, *then the solution* $(S_h(t) \geqslant 0, V_h(t) \geqslant 0, E_h(t) \geqslant 0, I_{hA}(t) \geqslant 0, I_h(t) \geqslant 0$ *and* $R_h(t) \geqslant 0)$ *of model (2.1) are positive* $\forall t > 0$

Proof. According to Asha and Nyimvua [12], Zenebe and Legese [13] and Rabiu et.al. [14], we proof the positivity of model (2.1) by contradiction. Given the non-negative initial conditions for $S_h(0), V_h(0), E_h(0), I_{hA}(0), I_h(0)$ and $R_h(0)$, the positivity of the system can be determined as follows: We make an assumption that there exists time t_i such that, $S_h(0) > 0, S_h(t_i) = 0, S_h'(t_i) < 0, V_h(t) > 0, E_h(t) > 0, I_{hA}(t) > 0, I_h(t) > 0, R_h(t) > 0$, for all $0 \leqslant t < t_i$.
In relation to our case and considering the first equation of the model (2.1), we have:

$$\frac{dS_h}{dt}(t_i) = \pi + \varphi V_h(t_i) + \tau R_h(t_i) - (\lambda + \mu + \theta)S_h(t_i)$$

Based on our assumption, this equation implies that:

$$\frac{dS_h}{dt}(t_i) = \pi + \varphi V_h(t_i) + \tau R_h(t_i) > 0$$

Table 2: Definition of model parameters

Variable	Definition
π	Recruitment rate into the susceptible population
μ	Natural death rate
β	COVID-19 transmission rate.
ξ	Modification factor for asymptomatic persons.
ϵ	Rate at which the exposed persons become symptomatic.
γ	Recovery rate of the symptomatic individuals.
δ	COVID-19 induced death rate for symptomatic individuals
ω	Rate at which exposed population become sick of COVID-19
φ	Rate of waning of COVID-19 vaccine-induced immunity
α	Rate of movement from asymptomatic infected class
κ	Rate of identification and treatment of the asymptomatic persons.
θ	Rate of vaccination of susceptible population.
τ	Rate at which recovered individual become susceptible

which is a contradiction. This indicates that $S_h(t) > 0$ for all $t > 0$. For the second equation, we have:

$$\frac{dV_h}{dt} = \theta S_h - (\varphi + \mu)V_h \geqslant -(\varphi + \mu)$$

Utilizing separation of variables and applying the initial conditions, solution to the above equation is: $V_h(t) \geqslant V_h(0)\exp(-(\mu+\varphi)t) \geqslant 0$ In the similar manner the equations three to equation six of the model (2.1) becomes:

$$\begin{aligned}
\frac{dE_h}{dt} &= \lambda S_h - (\omega + \mu)E_h \geqslant -(\omega + \mu)E_h \\
\frac{dI_{hA}}{dt} &= \omega(1-\epsilon)E_h - (\mu + \alpha)I_{hA} \geqslant -(\mu + \alpha)I_{hA} \\
\frac{dI_h}{dt} &= \omega\epsilon E_h + (1-\kappa)\alpha I_{hA} - (\mu + \delta + \gamma)I_h \geqslant -(\mu + \delta + \gamma)I_h \\
\frac{dR_h}{dt} &= \kappa\alpha I_{hA} + \gamma I_h - (\mu + \tau)R_h \geqslant -(\mu + \tau)R_h
\end{aligned}$$

whose solution are respectively given as:

$$\begin{aligned}
E_h(t) &= E_h(0)\exp(-(\mu+\omega)t) \geqslant 0 \quad \forall t > 0 \\
I_{hA}(t) &= I_{hA}(0)\exp(-(\mu+\alpha)t) \geqslant 0 \quad \forall t > 0 \\
I_h(t) &= I_h(0)\exp(-(\mu+\delta+\gamma)t) \geqslant 0 \quad \forall t > 0 \\
R_h(t) &= R_h(0)\exp(-(\mu+\tau)t) \geqslant 0 \quad \forall t > 0
\end{aligned}$$

This demonstrates that the solution of all state variables of the model are non-negative.

□

Invariant region
A population is said to be meaningful in biological sense if its global solution lies within an invariant region Ω [15, 16].

Theorem 2.2. *The solution set* $\{S_h(t), V_h(t), E_h(t), I_{hA}(t), I_h(t), R_h(t)\}$ *of the model (2.1) is confined to non-negative feasible region* Ω.

Proof. Consider the feasible region:
$\Omega = \{S_h(t), V_h(t), E_h(t), I_{hA}(t), I_h(t), R_h(t)\} \in \mathbb{R}^6_+ \quad \forall t \geqslant 0$. At any given time, the total population is given as:

$$N_h(t) = S_h(t) + V_h(t) + E_h(t) + I_{hA} + I_h(t) + R_h(t) \tag{2.2}$$

Differentiating equation (2.2) with respect to t gives:

$$\frac{dN_h}{dt} = \frac{dS_h}{dt} + \frac{dV_h}{dt} + \frac{dE_h}{dt} + \frac{dI_{hA}}{dt} + \frac{dI_h}{dt} + \frac{dR_h}{dt} \tag{2.3}$$

We now substitute model (2.1) into (2.3)

$$\begin{aligned}\frac{dN_h}{dt} &= [\pi + \tau R_h + \varphi V_n - (\lambda + \mu + \theta)S_h] + [\theta S_h - (\varphi + \mu)V_h] \\ &+ [\lambda S_h - (\omega + \mu)E_h] + [\omega(1-\epsilon)E_h - (\mu + \alpha)I_{hA}] \\ &+ [\omega\epsilon E_h + (1-\kappa)\alpha I_{hA} - (\mu + \delta + \gamma)I_h] \\ &+ [\kappa\alpha I_{hA} + \gamma I_h - (\mu + \tau)R_h]\end{aligned} \tag{2.4}$$

Expansion and simplification of equation (2.4) yields:

$$\frac{dN_h}{dt} = \pi - [S_h(t) + V_h(t) + E_h(t) + I_{hA} + I_h(t) + R_h(t)]\mu - \delta I_h \tag{2.5}$$

Substituting equation (2.2) to (2.5) gives:

$$\frac{dN_h}{dt} = \pi - \mu N_h - \delta I_h \leqslant \pi - \mu N_h \tag{2.6}$$

Evaluation of the equation (2.6) yields $N_h(t) \leqslant A\exp(-\mu t) + \frac{\pi}{\mu}$ which upon substituting the initial conditions, the above equation becomes:

$$N_h(t) \leqslant \frac{\pi}{\mu} + \left(\frac{\pi - \mu N_{h0}}{\mu}\right)\exp(-\mu t) \tag{2.7}$$

where $N_{h0} = N_h(0)$
This implies that:

$$\lim_{t\to\infty} \sup \quad N_h(t) \leqslant \frac{\pi}{\mu}$$

This shows that the positive solutions of the model (2.1) are bounded. Hence, the system under consideration is well posed mathematically and epidemiologically. □

Disease free equilibrium

The disease-free equilibrium (DFE) denoted as B_0 is a steady-state solution in which there is no COVID-19 infection in the community. Consequently, apart from the susceptible and the vaccinated, all other compartments are equated to zero. Thus $E_h = I_{hA} = I_h = R_h = 0$ and $\frac{dS_h^0}{dt} = \frac{dV_h^0}{dt} = 0$. Model equations (2.1) reduces to:

$$\begin{cases} \pi + \varphi V_h^0 - (\mu + \theta) S_h^0 = 0 \\ \theta S_h^0 - (\mu + \varphi) V_h^0 = 0 \end{cases} \tag{2.8}$$

Solving equation (2.8) simultaneously yields:

$$S_{h0} = \frac{\pi(\varphi + \mu)}{\mu(\varphi + \mu + \theta)} \quad \text{and} \quad V_{h0} = \frac{\pi\theta}{\mu(\varphi + \mu + \theta)} \tag{2.9}$$

Thus the DFE state, B_0, is given by:

$$(S_h^0, V_h^0, E_h^0, I_{hA}^0, I_h^0, R_h^0) = \left[\frac{\pi(\varphi + \mu)}{\mu(\varphi + \mu + \theta)}, \frac{\pi\theta}{\mu(\varphi + \mu + \theta)}, 0, 0, 0, 0 \right] \tag{2.10}$$

2.2. The basic reproduction number

The basic reproduction number is the number of cases that one COVID-19 case generates on average over its entire infectious period in an uninfected population [3]. We utilize the next generation matrix method [17] in the derivation of R_v for our dynamical system. In this method, the infected compartments are decomposed into two matrices F and V, where F represents the matrix containing the new infections elements and V is the matrix containing elements with transmission terms. The model (2.1) can be rewritten as:

$$\frac{d\chi}{dt} = F(\chi) - V(\chi) \tag{2.11}$$

More explicitly, the above equation can be written as:

$$\begin{pmatrix} \dot{E}_h \\ \dot{I}_{hA} \\ \dot{I}_h \end{pmatrix} = \begin{pmatrix} \beta(I_h + \xi I_{hA}) S_h \\ 0 \\ 0 \end{pmatrix} - \begin{pmatrix} (\omega + \mu) E_h \\ -\omega(1-\epsilon) E_h + (\mu + \alpha) I_h A \\ -\omega\epsilon E_h - (1-\kappa)\alpha I_h A + (\mu + \gamma + \delta) I_h \end{pmatrix}$$

Evaluation of the Jacobian of matrices F and V at the B_0 gives;

$$\mathcal{F} = \begin{pmatrix} 0 & \frac{\beta\xi\pi(\mu+\varphi)}{\mu(\mu+\theta+\varphi)} & \frac{\beta\pi(\mu+\varphi)}{\mu(\mu+\theta+\varphi)} \\ 0 & 0 & 0 \\ 0 & 0 & 0 \end{pmatrix}$$

and

$$\mathcal{V} = \begin{pmatrix} (\mu + \omega) & 0 & 0 \\ -\omega(1-\epsilon) & (\alpha + \mu) & 0 \\ -\epsilon\omega & -\alpha(1-\kappa) & (\mu + \gamma + \delta) \end{pmatrix}$$

The basic reproduction number is the spectral radius (The largest eigenvalue) of the next generation matrix $R_v = \rho(\mathcal{F}\mathcal{V}^{-1})$. By simple calculations, we can show that:

$$\mathcal{V}^{-1} = \begin{pmatrix} \frac{1}{\mu+\omega} & 0 & 0 \\ \frac{\omega(1-\epsilon)}{(\alpha+\mu)(\omega+\mu)} & \frac{1}{\alpha+\mu} & 0 \\ \frac{\alpha\kappa\omega(1-\epsilon)+\omega(\alpha+\mu\varepsilon)}{(\mu+\omega)(\alpha+\mu)(\mu+\delta+\gamma)} & \frac{\alpha(1-\kappa)}{(\alpha+\mu)(\mu+\delta+\gamma)} & \frac{1}{\mu+\delta+\gamma} \end{pmatrix} \tag{2.12}$$

This gives:

$$\mathcal{F}\mathcal{V}^{-1} = \begin{pmatrix} a_{11} & a_{12} & a_{13} \\ 0 & 0 & 0 \\ 0 & 0 & 0 \end{pmatrix}$$

Where:

$$a_{11} = \frac{\pi\beta\omega(\mu+\varphi)\{\xi(1-\epsilon)(\mu+\delta+\gamma)+\alpha(1-\kappa)+\epsilon(\alpha\kappa+\mu)\}}{\mu(\mu+\omega)(\mu+\alpha)(\mu+\theta+\varphi)(\mu+\gamma+\delta)}$$
$$a_{12} = \frac{\pi\beta(\mu+\varphi)[\xi(\mu+\gamma+\delta)+\alpha(1-\kappa)]}{\mu(\mu+\alpha)(\mu+\gamma+\delta)(\mu+\theta+\varphi)}$$
$$a_{13} = \frac{\pi\beta(\mu+\varphi)}{\mu(\mu+\theta+\varphi)(\mu+\gamma+\delta)}$$

The basic reproduction number plays a pivotal role when analyzing any epidemiological model. The effective reproduction of our dynamical system is thus:

$$R_v = \frac{\pi\beta\omega(\mu+\varphi)\{\xi(1-\epsilon)(\mu+\delta+\gamma)+\alpha(1-k)+\epsilon(\alpha\kappa+\mu)\}}{\mu(\mu+\omega)(\mu+\alpha)(\mu+\theta+\varphi)(\mu+\gamma+\delta)} \tag{2.13}$$

For clear interpretation of the above reproduction number, we can separate this expression of R_v as follows:

$$R_v = R_A + R_S$$

Where

$$R_A = \frac{\pi\beta\omega(\mu+\varphi)\xi(1-\epsilon)}{\mu(\mu+\omega)(\mu+\alpha)(\mu+\theta+\varphi)} \tag{2.14}$$

R_A represents the probability of the total population becoming asymptomatic upon infection times the mean exposed, asymptomatic and the vaccinated population.

$$R_S = \frac{\pi\beta\omega(\mu+\varphi)\{\alpha(1-k)+\epsilon(\alpha\kappa+\mu)\}}{\mu(\mu+\omega)(\mu+\alpha)(\mu+\theta+\varphi)(\mu+\gamma+\delta)} \tag{2.15}$$

R_S represents the probability of total population becoming symptomatic upon infection multiplied by mean exposed, asymptomatic, symptomatic and vaccinated population.
The analytically generated R_v from our model thus points to the fact that the presence of both symptomatic and asymptomatic persons could drive the growth of COVID-19 in the general population.

We note that for the case where vaccination has not been rolled out equation (2.13) reduces to:

$$R_0 = \frac{\pi\beta\omega\{\xi(1-\epsilon)(\mu+\delta+\gamma)+\alpha(1-k)+\epsilon(\alpha\kappa+\mu)\}}{\mu(\mu+\omega)(\mu+\alpha)(\mu+\gamma+\delta)} \tag{2.16}$$

2.3. The stability of disease free equilibrium (DFE)

In this section, we explore the local and global stability of model (2.1) at DFE by utilizing the following theorems:

Theorem 2.3. *The disease-free state,* B_0*, of the model (2.1) is locally asymptotically stable(LAS) when* $R_v < 1$ *and unstable if* $R_v > 1$.

Proof. The local stability of the model is determined by first evaluating the Jacobian matrix at DFE state B_0 which gives:

$$J_{B_0} = \begin{pmatrix} -(\mu+\theta) & \varphi & 0 & -\frac{\beta\xi(\varphi+\mu)\pi}{\mu(\mu+\varphi+\theta)} & -\frac{\beta(\varphi+\mu)\pi}{\mu(\mu+\varphi+\theta)} & \tau \\ \theta & -(\mu+\varphi) & 0 & 0 & 0 & 0 \\ 0 & 0 & -(\mu+\omega) & \frac{\beta\xi\pi(\varphi+\mu)}{\mu(\mu+\varphi+\theta)} & \frac{\beta\pi(\varphi+\mu)}{\mu(\mu+\varphi+\theta)} & 0 \\ 0 & 0 & \omega(1-\epsilon) & -(\alpha+\mu) & 0 & 0 \\ 0 & 0 & \epsilon\omega & \alpha(1-\kappa) & -(\mu+\gamma+\delta) & 0 \\ 0 & 0 & 0 & \alpha\kappa & \gamma & -(\mu+\tau) \end{pmatrix} \tag{2.17}$$

From the Jacobian matrix equation (2.17), we make use of the trace-determinant method so as to proof the local stability of B_0. For local asymptotic stability, the following Routh-Hurwitz conditions have to be satisfied:

(i) $TrJ(B_0) < 0$

(ii) $DetJ(B_0) > 0$

Thus:

$$\begin{cases} TrJ(B_0) = -(\mu+\theta+\mu+\varphi+\mu+\omega+\mu+\alpha+\mu+\gamma+\delta+\mu+\tau) \\ \quad = -(6\mu+\theta+\varphi+\omega+\alpha+\gamma+\delta+\tau) < 0 \end{cases} \tag{2.18}$$

Due to the complexity of the matrix space involved, we utilize python programming language to determine the determinant of $J(B_0)$. This gives:

$$\begin{cases} DetJ(B_0) = -\mu(\mu+\tau)(\mu+\theta+\varphi)\{-(\mu+\omega)(\alpha+\mu)(\mu+\gamma+\delta) \\ +\frac{\beta\pi\omega(\varphi+\mu)}{\mu(\mu+\varphi+\theta)}[\xi(1-\epsilon)(\mu+\gamma+\delta)+\alpha(1-\kappa)+\epsilon(\alpha\kappa+\mu)]\} \end{cases} \tag{2.19}$$

Through further simplification and utilization of equation (2.13), equation (2.19) becomes:

$$DetJ(B_0) = \mu(\mu+\tau)(\mu+\theta+\varphi)(\mu+\omega)(\mu+\alpha)(\mu+\gamma+\delta)(1-R_v) \tag{2.20}$$

Where R_v is the effective reproduction number.

For determinant $DetJ(B_0) > 0$, it follows that $R_v < 1$. Hence the disease-free equilibrium (B_0) of model (2.1) is locally asymptotically stable if $R_v < 1$ and unstable if $R_v > 1$. □

The implication of the above theorem is that the extinction of disease in population is possible for $R_v < 1$, but if $R_v > 1$, the ballooning of infection cases in the population is assured.

For the next theorem, we investigate the global stability of DFE by using Lyapunov function technique [18].

Theorem 2.4. *The COVID-19-free equilibrium point* B_0 *of model (2.1) is globally asymptotically stable in the region* Ω *if* $R_v \leqslant 1$ *and unstable if* $R_v > 1$.

Proof. Let L be a Lyapunov function with positive constants c_1, c_2, c_3 and c_4 such that:

$$\begin{cases} L = (S_h - S_h^0 - S_h^0 \ln \frac{S_h}{S_h^0}) + (V_h - V_h^0 - V_h^0 \ln \frac{V_h}{V_h^0}) + c_1 E_h \\ \quad + c_2 I_{hA} + c_3 I_h + c_4 R_h \end{cases} \tag{2.21}$$

Differentiating the above Lyapunov equation with respect to time gives:

$$\begin{cases} \frac{dL}{dt} = (1 - \frac{S_h^0}{S_h}) \frac{dS_h}{dt} + (1 - \frac{V_h^0}{V_h}) \frac{dV_h}{dt} + c_1 \frac{dE_h}{dt} \\ \quad + c_2 \frac{dI_{hA}}{dt} + c_3 \frac{dI_h}{dt} + c_4 \frac{dR_h}{dt} \end{cases} \tag{2.22}$$

Substituting model (2.1) into (2.22) yields:

$$\begin{cases} \frac{dL}{dt} = (1 - \frac{S_h^0}{S_h})[\pi + \varphi V_h + \tau R_h - \lambda S_h - (\mu + \theta) S_h] \\ \quad + (1 - \frac{V_h^0}{V_h})[\theta S_h - (\mu + \varphi) V_h] + c_1[\lambda S_h - (\mu + \omega) E_h] \\ \quad + c_2[(1 - \epsilon)\omega E_h - (\mu + \alpha) I_{hA}] + c_3[\epsilon\omega E_h + (1 - \kappa)\alpha I_{hA} - (\mu + \gamma + \delta) I_h] \\ \quad + c_4[\alpha\kappa I_{hA} + \gamma I_h - (\mu + \tau) R_h] \end{cases} \tag{2.23}$$

Suppose $S_h \leqslant S_h^0 = \frac{\pi(\mu+\varphi)}{\mu(\mu+\theta+\varphi)}$ and $V_h \leqslant V_h^0 = \frac{\pi\theta}{\mu(\mu+\theta+\varphi)}$, and upon substituting $\lambda = \beta(\xi I_{hA} + I_h)$ to equation (2.23) yields:

$$\begin{cases} \frac{dL}{dt} \leqslant c_1[\frac{\pi(\mu+\varphi)\beta(\xi I_{hA} + I_h)}{\mu(\mu+\theta+\varphi)} - (\mu + \omega) E_h] \\ \quad + c_2[(1 - \epsilon)\omega E_h - (\mu + \alpha) I_{hA}] \\ \quad + c_3[\epsilon\omega E_h + (1 - \kappa)\alpha I_{hA} - (\mu + \gamma + \delta) I_h] \\ \quad + c_4[\alpha\kappa I_{hA} + \gamma I_h - (\mu + \tau) R_h] \end{cases} \tag{2.24}$$

The above equation implies that:

$$\begin{cases} \frac{dL}{dt} \leqslant [-(\mu + \omega)c_1 + \omega(1 - \epsilon)c_2 + \epsilon\omega c_3] E_h \\ \quad + [\frac{\pi\beta\xi(\mu+\varphi)}{\mu(\mu+\theta+\varphi)} c_1 - (\mu + \alpha)c_2 + \alpha(1 - \kappa)c_3 + \alpha\kappa c_4] I_{hA} \\ \quad + [\frac{\pi\beta(\mu+\varphi)}{\mu(\mu+\theta+\varphi)} c_1 - (\mu + \gamma + \delta)c_3 + \gamma c_4] I_h - (\mu + \tau)c_5 R_h \end{cases} \tag{2.25}$$

Equating the coefficients of E_h, I_{hA}, I_h, J_h and R_h to zero gives:

$$c_1 = (\mu + \gamma + \delta),\ c_2 = \frac{\mu(\mu+\omega)(\mu+\theta+\varphi)(\mu+\gamma+\delta) - \pi\epsilon\omega\beta(\mu+\varphi)}{\mu\omega(1-\epsilon)(\mu+\theta+\varphi)}$$
$$c_3 = \frac{\beta\pi(\mu+\varphi)}{\mu(\mu+\theta+\varphi)},\ c_4 = c_5 = 0$$

We thus obtain:

$$\frac{dL}{dt} \leqslant \frac{(\mu + \omega)(\mu + \alpha)(\mu + \gamma + \delta)}{\omega(1 - \epsilon)} (R_v - 1) I_{hA} \tag{2.26}$$

Its worth noting that: $\frac{dL}{dt} \leqslant 0$, if $R_v \leqslant 1$ and $\frac{dL}{dt} = 0$ iff $I_{hA} = 0$. Thus, plugging $E_h = I_{hA} = I_h = R_h = 0$ into model (2.1) points to the fact that $S_h(t) \rightarrow$

$\frac{\pi(\mu+\varphi)}{\mu(\mu+\theta+\varphi)}$ and $V_h(t) \to \frac{\pi\theta}{\mu(\mu+\theta+\varphi)}$ as $t \to \infty$. Hence the largest compact invariant set in $\{(S_h, V_h, E_h, I_{hA}, I_h, R_h) \in \Omega; \frac{dL}{dt} \leqslant 0\}$, is the singleton set B_0. Thus from LaSalle's invariance principle [19], we make the conclusion that the COVID-19 free equilibrium point is globally asymptotically stable in Ω if $R_v < 1$.
The explanation above points to the fact that COVID-19 infection can be abased in the general population if and only if $R_v < 1$. □

2.4. Existence of an endemic equilibrium

We endeavor to investigate the existence of endemic equilibrium, B_e of the model (2.1) in this subsection.

Theorem 2.5. *If $R_v > 1$, there exists a unique endemic equilibrium $B_e = (S_h^*, V_h^*, E_h^*, I_{hA}^*, I_h^*, R_h^*)$ of the model (2.1). The endemic equilibrium does not exist for $R_v < 1$.*

Proof. For the existence of endemic equilibrium, we equate the right side of the model (2.1) to zero and then solve.

$$\begin{cases} \pi + \tau R_h^* + \varphi V_h^* - \beta(I_h^* + \xi I_{hA}^*)S_h^* - (\mu+\theta)S_h^* = 0 \\ \theta S_h^* - (\varphi+\mu)V_h^* = 0 \\ \omega(1-\epsilon)E_h^* - (\mu+\alpha)I_{hA}^* = 0 \\ \beta(I_h^* + \xi I_{hA}^*)S_h^* - (\omega+\mu)E_h^* = 0 \\ \omega\epsilon E_h^* + (1-\kappa)\alpha I_{hA}^* - (\mu+\delta+\gamma)I_h^* = 0 \\ \kappa\alpha I_{hA}^* + \gamma I_h^* - (\mu+\tau)R_h^* = 0 \end{cases} \tag{2.27}$$

Solution to the above system gives rise to the following:

$$\begin{aligned} S_h^* &= \frac{\pi(\mu+\varphi)}{\mu(\mu+\theta+\varphi)R_v} \\ V_h^* &= \frac{\pi\theta}{\mu(\mu+\theta+\varphi)R_v} \\ E_h^* &= \frac{\pi\Phi_1\Phi_2\Phi_3(R_v-1)}{\{(\mu+\omega)\Phi_1\Phi_2\Phi_3 - \tau\omega(\Phi_3\Phi_5+\gamma\Phi_4)\}R_v} \\ I_{hA}^* &= \frac{\pi\omega\Phi_2\Phi_3\Phi_5(R_v-1)}{\alpha\kappa\{(\mu+\omega)\Phi_1\Phi_2\Phi_3 - \tau\omega(\Phi_3\Phi_5+\gamma\Phi_4)\}R_v} \\ I_h^* &= \frac{\pi\omega\Phi_4\Phi_2(R_v-1)}{\{(\mu+\omega)\Phi_1\Phi_2\Phi_3 - \tau\omega(\Phi_3\Phi_5+\gamma\Phi_4)\}R_v} \\ R_h^* &= \frac{\pi\omega(R_v-1)(\Phi_3\Phi_5+\gamma\Phi_4)}{\{(\mu+\omega)\Phi_1\Phi_2\Phi_3 - \tau\omega(\Phi_3\Phi_5+\gamma\Phi_4)\}R_v} \end{aligned}$$

where $\Phi_1 = (\mu+\alpha)$, $\Phi_2 = (\mu+\tau)$, $\Phi_3 = (\mu+\delta+\gamma)$, $\Phi_4 = \alpha(1-\kappa) + \epsilon(\alpha\kappa+\mu)$ and $\Phi_5 = \alpha\kappa(1-\epsilon)$. Substitution of the values of $\Phi_1, \Phi_2, \Phi_3, \Phi_4$ and Φ_5 in $\{(\mu+\omega)\Phi_1\Phi_2\Phi_3 - \tau\omega(\Phi_3\Phi_5+\gamma\Phi_4)\}$ and then simplification yields:

$$\begin{aligned} \{(\mu+\omega)\Phi_1\Phi_2\Phi_3 - \tau\omega(\Phi_3\Phi_5+\gamma\Phi_4)\} = \mu^2\{\Phi_1(\omega+\tau+\Phi_3) + \omega\tau + (\delta+\gamma)(\omega+\tau)\} + \\ \tau\omega\alpha(\mu+\delta)(\epsilon\kappa+(1-\kappa)) + \mu\omega(\tau\gamma(1-\epsilon) + \delta(\alpha+\tau)) + \mu\alpha\gamma(\omega+\tau). \end{aligned}$$

Since $\epsilon < 1$ and also $\kappa < 1$, $\{(\mu+\omega)\Phi_1\Phi_2\Phi_3 - \tau\omega(\Phi_3\Phi_5 + \gamma\Phi_4)\} > 0$.
It can therefore be observed that if $R_v = 1$, we obtain the COVID-19 free equilibrium point. The unique endemic equilibrium in Ω exists if $E_h^* > 0$, $I_{Ah}^* > 0$, $I_h^* > 0$ and $R_h^* > 0$. This is actualized if and only if $(R_v - 1) > 0$ and no endemic equilibrium when $(R_v - 1) < 0$. □

2.5. Bifurcation analysis

In this subsection we investigate the nature of bifurcation by utilizing Theorem 4.1 from [20] which is based on the center manifold theory [21]. In this theory, there are two important coefficients, say, a and b, that dictate the dynamics of the system on the center manifold. In particular, if $a < 0$ and $b > 0$, then the nature of bifurcation is forward while if $a > 0$ and $b > 0$, then the bifurcation is backward.

This is done by first letting the coefficient of transmission β to be the bifurcation parameter. This is done by solving $R_v = 1$ to obtain:

$$\beta = \beta^* = \frac{\mu(\mu+\omega)(\mu+\alpha)(\mu+\theta+\varphi)(\mu+\delta+\gamma)}{\pi\omega(\mu+\varphi)\{\xi(1-\epsilon)+\alpha(1-\kappa)+\epsilon(\alpha\kappa+\mu)\}}$$

The Jacobian matrix J_{B_0,β^*} for model 1 evaluated at disease-free equilibrium where β is substituted with the value of β^*, has one of the eigenvalues being zero(0) while the other five eigenvalues have negative sign. This implies that B_0 is a non-hyperbolic equilibrium at $\beta = \beta^*$. The presence of a simple zero eigenvalues permits us to utilize center manifold theory to establish the local stability of endemic equilibrium B_e. Evaluating the right eigenvector $W = (w_1, w_2, w_3, w_4, w_5, w_6)^T$ and left eigenvector $V = (v_1, v_2, v_3, v_4, v_5, v_6)^T$ associated to the zero eigenvalues give:

$$w_1 = -\frac{(\mu+\varphi)w_6(\frac{A}{w_6}-\tau)}{\mu(\mu+\theta+\varphi)}, \quad w_2 = -\frac{\theta w_6(\frac{A}{w_6}-\tau)}{\mu(\mu+\theta+\varphi)}$$

where $A = \frac{(\mu+\omega)(\mu+\alpha)\{\xi(1-\epsilon)(\mu+\gamma+\delta)+\alpha(1-\kappa)+\epsilon(\mu+\alpha\kappa)\}}{\xi(1-\epsilon)+\alpha(1-\kappa)+\epsilon(\mu+\alpha\kappa)}$

$$w_3 = \mu+\alpha, \quad w_4 = \omega(1-\epsilon), \quad w_5 = \frac{\omega\{\epsilon(\mu+\alpha\kappa)+\alpha(1-\kappa)\}}{\mu+\gamma+\delta}, \quad w_6 = \alpha\kappa(1-\epsilon)\omega + \gamma w_5$$

and
$v_1 = v_2 = v_6 = 0$, $v_3 = \frac{\omega\{\xi(1-\epsilon)+\alpha(1-\kappa)+\epsilon(\mu+\alpha\kappa)\}v_5}{(\mu+\omega)(\mu+\alpha)}$, $v_4 = \frac{\{\xi+\alpha(1-\kappa)\}v_5}{\mu+\alpha}$ and $v_5 = \frac{1}{c_1+c_2+w_5}$ where $c_1 = \frac{\omega\{\xi(1-\epsilon)+\alpha(1-\kappa)+\epsilon(\mu+\alpha\kappa)\}}{\mu+\omega}$ and $c_2 = \frac{\omega(1-\epsilon)\{\xi+\alpha(1-\kappa)\}}{\mu+\alpha}$ We now calculate the bifurcation constants a and b where:

$$a = \sum_{k,i,j=1}^{6} v_k w_i w_j \frac{\partial^2 f_k}{\partial x_i \partial x_j}(B_0, \beta^*)$$

$$b = \sum_{k,i,j=1}^{6} v_k w_i \frac{\partial^2 f_k}{\partial x_i \partial \beta}(B_0, \beta^*)$$

For simplicity and ease in algebraic manipulations, we re-write the state variables of our model (2.1) as follows: $S_h = x_1$, $V_h = x_2$, $E_h = x_3$, $I_{hA} = x_4$, $I_h = x_5$ and $R_h = x_6$. We further define equation $\frac{dX}{dt} = F(x)$ where $X = (x_1, x_2, x_3, x_4, x_5, x_6)$ and

$F = (f_1, f_2, f_3, f_3, f_4, f_5, f_6)$. We consider the nonzero second order partial derivatives which gives;

$$\begin{cases} \nu_3 w_1 w_4 \frac{\partial^2 f_3}{\partial x_1 \partial x_4} = -\nu_3 \frac{(\mu+\varphi) w_6 \{\frac{A}{w_6} - \tau\}}{\mu(\mu+\theta+\varphi)} w_4 \beta^* \xi \\ \nu_3 w_4 w_1 \frac{\partial^2 f_3}{\partial x_4 \partial x_1} = -\nu_3 w_4 \frac{(\mu+\varphi) w_6 \{\frac{A}{w_6} - \tau\}}{\mu(\mu+\theta+\varphi)} \beta^* \xi \\ \nu_3 w_1 w_5 \frac{\partial^2 f_3}{\partial x_1 \partial x_5} = -\nu_3 \frac{(\mu+\varphi) w_6 \{\frac{A}{w_6} - \tau\}}{\mu(\mu+\theta+\varphi)} w_5 \beta^* \\ \nu_3 w_5 w_1 \frac{\partial^2 f_3}{\partial x_1 \partial x_5} = -\nu_3 w_5 \frac{(\mu+\varphi) w_6 \{\frac{A}{w_6} - \tau\}}{\mu(\mu+\theta+\varphi)} \beta^* \end{cases} \tag{2.28}$$

The summing up equations (2.28) gives the value of a as:

$$a = -2\nu_3 \frac{(\mu+\varphi) w_6 \{\frac{A}{w_6} - \tau\}}{\mu(\mu+\theta+\varphi)} \beta^* (\xi w_4 + w_5) \tag{2.29}$$

In the same manner we determine the value of b as:

$$\begin{cases} \nu_3 w_4 \frac{\partial^2 f_3}{\partial x_4 \partial \beta^*} = \nu_3 w_4 \frac{\pi(\mu+\varphi)}{\mu(\mu+\theta+\varphi)} \\ \nu_3 w_5 \frac{\partial^2 f_3}{\partial x_5 \partial \beta^*} = \nu_3 w_5 \xi \frac{\pi(\mu+\varphi)}{\mu(\mu+\theta+\varphi)} \end{cases} \tag{2.30}$$

The sum of the equations in (2.30) gives the value of b as:

$$b = \nu_3 \frac{\pi(\mu+\varphi)}{\mu(\mu+\theta+\varphi)} (w_4 \xi + w_5) > 0 \tag{2.31}$$

None negativity of b implies that direction of bifurcation at $R_\nu = 1$ is entirely determined by the sign of a which depends on the re-infection rate τ. For backward bifurcation,

$$\tau > \frac{(\mu+\gamma+\delta)(\mu+\omega)(\mu+\alpha)(\xi(1-\epsilon)\omega + w_5)}{(\xi(1-\epsilon)\omega + (\mu+\gamma+\delta)w_5)(\alpha\kappa(1-\epsilon)\omega + \gamma w_5)} \tag{2.32}$$

Theorem 2.6. *The model (2.1) undergoes backward bifurcation at* $R_\nu = 1$ *whenever inequality (2.32) holds.*

The above theorem is in conformity with study by Kassa et.al.[7] that suggested that backward bifurcation is possible if the recovered individuals do not gain permanent immunity to infections regardless of the COVID-19 variant. Moreover, it is note worthy that for the case where the recovered persons acquires permanent immunity to COVID-19 infection (i.e $\tau = 0$), the bifurcation coefficient a becomes:

$$a = -2\nu_3 \frac{(\mu+\omega)(\mu+\alpha)(\mu+\varphi)(\mu+\gamma+\delta)(\xi(1-\epsilon)\omega + w_5)}{\mu(\mu+\theta+\varphi)[\xi(1-\epsilon)\omega + (\mu+\gamma+\delta)w_5]} \beta^* (\xi w_4 + w_5) < 0$$

This rules out the occurrence of backward bifurcation but instead, forward bifurcation sets in. Hence we obtain the following conclusion:

Theorem 2.7. *(Local stability of endemic equilibrium). The unique endemic equilibrium* B_e *of model (2.1) is locally asymptotically stable (LAS) if* $R_\nu > 1$.

2.6. Global stability of COVID-19 endemic equilibrium point

Theorem 2.8. *The unique endemic equilibrium* B_e *of the model (2.1) is globally asymptotically stable in* Ω *whenever* $R_v > 1$.

Proof. Let c_1, c_2, c_3, c_4, c_5 and c_6 be non-negative constants and with no loss of generality, we consider a special case of our system where $\varphi = 0$ and $\tau = 0$. We consider a Lyapunov function defined as:

$$L = c_1L_1 + c_2L_2 + c_3L_3 + c_4L_4 + c_5L_5 + c_6L_6$$

where

$$\begin{cases} L_1 = S_h^{**}.g\left(\frac{S_h}{S_h^{**}}\right),\ L_2 = V_h^{**}.g\left(\frac{V_h}{V_h^{**}}\right),\ L_3 = E_h^{**}.g\left(\frac{E_h}{E_h^{**}}\right), \\ L_4 = I_{hA}^{**}.g\left(\frac{I_{hA}}{I_{hA}^{**}}\right),\ L_5 = I_h^{**}.g\left(\frac{I_h}{I_h^{**}}\right),\ L_6 = R_h^{**}.g\left(\frac{R_h}{R_h^{**}}\right). \end{cases} \tag{2.33}$$

and that $g(x) = x - 1 - \ln x \geqslant g(1) = 0$ for any $x > 0$
Differentiating L with respect to t gives:

$$\begin{cases} \frac{dL}{dt} = c_1\left(1 - \frac{S_h^{**}}{S_h}\right)\left\{\pi - \beta(\xi I_{hA} + I_h)S_h - (\mu + \theta)S_h\right\} \\ \quad + c_2\left(1 - \frac{V_h^{**}}{V_h}\right)\left\{\theta S_h - \mu V_h\right\} \\ \quad + c_3\left(1 - \frac{E_h^{**}}{E_h}\right)\left\{\beta(\xi I_{hA} + I_h)S_h - (\mu + \omega)E_h\right\} \\ \quad + c_4\left(1 - \frac{I_{hA}^{**}}{I_{hA}}\right)\left\{\omega(1-\epsilon)E_h - (\mu + \alpha)I_{hA}\right\} \\ \quad + c_5\left(1 - \frac{I_h^{**}}{I_h}\right)\left\{\omega\epsilon E_h + (1-\kappa)\alpha I_{hA} - (\mu + \delta + \gamma)I_h\right\} \\ \quad + c_6\left(1 - \frac{R_h^{**}}{R_h}\right)\left\{\kappa\alpha I_{hA} + \gamma I_h - \mu R_h\right\} \end{cases} \tag{2.34}$$

At steady endemic equilibrium,

$$\begin{cases} \pi = \beta(\xi I_{hA}^{**} + I_h^{**})S_h^{**} + (\mu + \theta)S_h^{**},\ \theta = \frac{\mu V_h^{**}}{S_h^{**}}, \\ (\mu + \omega) = \frac{\beta(\xi I_{hA}^{**} + I_h^{**})S_h^{**}}{E_h^{**}},\ (\mu + \alpha) = \frac{\omega(1-\epsilon)E_h^{**}}{I_{hA}^{**}}, \\ (\mu + \delta + \gamma) = \frac{\omega\epsilon E_h^{**} + (1-\kappa)\alpha I_{hA}^{**}}{I_h^{**}},\ \mu = \frac{\kappa\alpha I_{hA}^{**} + \gamma I_h}{R_h^{**}}. \end{cases} \tag{2.35}$$

Substituting (2.35) into (2.34) gives,

$$\begin{cases} \frac{dL}{dt} = c_1\left(1 - \frac{S_h^{**}}{S_h}\right)\left\{\beta\xi S_h^{**}I_{hA}^{**}\left(1 - \frac{S_hI_{hA}}{S_h^{**}I_{hA}^{**}}\right) + \beta S_h^{**}I_h^{**}\left(1 - \frac{S_hI_h}{S_h^{**}I_h^{**}}\right)\right. \\ \quad \left. + (\mu + \theta)S_h^{**}\left(1 - \frac{S_h}{S_h^{**}}\right)\right\} + c_2\left(1 - \frac{V_h^{**}}{V_h}\right)\left\{\mu V_h^{**}\left(\frac{S_h}{S_h^{**}} - \frac{V_h}{V_h^{**}}\right)\right\} \\ \quad + c_3\left(1 - \frac{E_h^{**}}{E_h}\right)\left\{\beta\xi S_h^{**}I_{hA}^{**}\left(\frac{S_hI_{hA}}{S_h^{**}I_{hA}^{**}} - \frac{E_h}{E_h^{**}}\right) + \beta S_h^{**}I_h^{**}\left(\frac{S_hI_h}{S_h^{**}I_h^{**}} - \frac{E_h}{E_h^{**}}\right)\right\} \\ \quad + c_4\left(1 - \frac{I_{hA}^{**}}{I_{hA}}\right)\left\{\omega(1-\epsilon)E_h^{**}\left(\frac{E_h}{E_h^{**}} - \frac{I_{hA}}{I_{hA}^{**}}\right)\right\} \\ \quad + c_5\left(1 - \frac{I_h^{**}}{I_h}\right)\left\{\omega\epsilon\left(\frac{E_h}{E_h^{**}} - \frac{I_h}{I_h^{**}}\right) + (1-\kappa)\alpha I_{hA}^{**}\left(\frac{I_{hA}}{I_h^{**}} - \frac{I_h}{I_h^{**}}\right)\right\} \\ \quad + c_6\left(1 - \frac{R_h^{**}}{R_h}\right)\left\{\kappa\alpha I_{hA}^{**}\left(\frac{I_{hA}}{I_{hA}^{**}} - \frac{R_h}{R_h^{**}}\right) + \gamma I_h^{**}\left(\frac{I_h}{I_h^{**}} - \frac{R_h}{R_h^{**}}\right)\right\} \end{cases} \tag{2.36}$$

Upon simplification, the above equation becomes:

$$\begin{cases} \frac{dL}{dt} = -\frac{c_1 S_h^{**}}{S_h}(\mu+\theta)\left(\frac{S_h}{S_h^{**}}-1\right)^2 + c_1\beta\xi S_h^{**} I_{hA}^{**}\left\{3-\frac{S_h^{**}}{S_h}-\frac{E_h I_{hA}^{**}}{E_h^{**} I_{hA}}-\frac{S_h E_h^{**} I_{hA}}{S_h^{**} E_h I_{hA}^{**}}\right\} \\ \quad +c_1\beta S_h^{**} I_h^{**}\left\{3-\frac{S_h^{**}}{S_h}-\frac{E_h I_h^{**}}{E_h^{**} I_h}-\frac{S_h E_h^{**} I_h}{S_h^{**} E_h I_h^{**}}\right\}+c_2\mu V_h^{**}\left\{1-\frac{V_h}{V_h^{**}}-\frac{S_h}{S_h^{**}}\left(\frac{V_h^{**}}{V_h}-1\right)\right\} \\ \quad +c_5(1-\kappa)\alpha I_{hA}^{**}\left\{1-\frac{I_h}{I_h^{**}}-\frac{I_{hA}}{I_{hA}^{**}}\left(\frac{I_h^{**}}{I_h}-1\right)\right\} \\ \quad +c_6\kappa\alpha I_{hA}^{**}\left\{1-\frac{R_h}{R_h^{**}}-\frac{I_{hA}}{I_{hA}^{**}}\left(\frac{R_h^{**}}{R_h}-1\right)\right\}+c_6\gamma I_h^{**}\left\{1-\frac{R_h}{R_h^{**}}-\frac{I_h}{I_h^{**}}\left(\frac{R_h^{**}}{R_h}-1\right)\right\} \end{cases} \tag{2.37}$$

Finally, since the arithmetic mean is greater or equal to the geometric mean as applied by [22, 23, 24], it follows that:

$$\begin{gathered} \left(3-\frac{S_h^{**}}{S_h}-\frac{E_h I_{hA}^{**}}{E_h^{**} I_{hA}}-\frac{S_h E_h^{**} I_{hA}}{S_h^{**} E_h I_{hA}^{**}}\right)\leqslant 0,\ \left(3-\frac{S_h^{**}}{S_h}-\frac{E_h I_h^{**}}{E_h^{**} I_h}-\frac{S_h E_h^{**} I_h}{S_h^{**} E_h I_h^{**}}\right)\leqslant 0 \\ \left\{1-\frac{V_h}{V_h^{**}}-\frac{S_h}{S_h^{**}}\left(\frac{V_h^{**}}{V_h}-1\right)\right\}\leqslant 0,\ \left\{1-\frac{I_h}{I_h^{**}}-\frac{I_{hA}}{I_{hA}^{**}}\left(\frac{I_h^{**}}{I_h}-1\right)\right\}\leqslant 0 \\ \left\{1-\frac{R_h}{R_h^{**}}-\frac{I_{hA}}{I_{hA}^{**}}\left(\frac{R_h^{**}}{R_h}-1\right)\right\}\leqslant 0,\ \left\{1-\frac{R_h}{R_h^{**}}-\frac{I_h}{I_h^{**}}\left(\frac{R_h^{**}}{R_h}-1\right)\right\}\leqslant 0 \end{gathered}$$

The non-negativity of the system parameters permits us to make conclusion that $\frac{dL}{dt}\leqslant 0$ for $R_v > 1$. Moreover, the set where $\frac{dF}{dt}=0$ is $\Omega=\{(S_h,V_h,E_h,I_{hA},I_h,R_h): S_h = S_h^{**},\ V_h = V_h^{**},\ E_h = E_h^{**},\ I_{hA} = I_{hA}^{**},\ I_h = I_h^{**},\ R_h = R_h^{**}\}$, and by LaSalle's Invariance Principle [25], the only compact invariant set of Ω is the singleton set B_e. Thus the endemic equilibrium B_e is globally asymptotically stable. This completes the proof. □

3. Model fitting to COVID-19 data for Kenya

In this section, we estimate parameters used in the model (2.1) based on monthly cumulative COVID-19 data for confirmed infective cases in Kenya from the 30th day of March, 2020 until March 31st March 2022 (see table (3)). The data is obtained from the worldmeters and can be accessed via the link given in [26]. This corresponds to the period when the corona cases in Kenya, just like the rest of the countries in the world, were growing at an alarming rate. It is worth noting that for the purpose of model fitting, the model system is reduced to a simpler version, but at the same time ensuring key population classes are maintained. We consider both θ and φ to be equal to zero which implies that the vaccinated class is ignored during the curve fitting. The time unit considered in the model versus data fitting is a unit per month. The average life expectancy of Kenyans in 2022 was 67.21 years [27]. The estimate of the natural death rate is obtained by taking the reciprocal of the life expectancy per month, i.e $\frac{1}{67.12\times 12}$, an approach utilized in [28].

The recruitment rate into susceptible population for our mass action model is obtained by utilizing the approach employed in [29]and [30] i.e, $\pi = \frac{1000}{67.21\times 12}$. The latent period for COVID-19 ranges from five to seven days, thus we take $\omega = 1/7$ [31]. To obtain the numerical values of the rest of the parameters, we fit the COVID-19 data using nonlinear least-square curve fitting method embedded in lmfit python package [32].

According to Corona virus Pandemic in Kenya report [26], there have been 50 COVID-19 reported cases as at March 30th 2020. We take the initial value of symptomatic individuals to be $I_h(0) = 50$. Kenya, just like any other third world countries experienced some challenges in conducting tests to the general population due to the limited resources

Table 3: Monthly cumulative COVID-19 cases

Month	Confirmed cases	Month	Confirmed cases
Mar. 30, 2020	50	April 28, 2021	157492
April 29, 2020	374	May 30, 2021	170647
May 29, 2020	1618	June 29, 2021	182884
June 29, 2020	6070	July 30, 2021	201009
July 29, 2020	19125	Aug. 29, 2021	234589
Aug. 30, 2020	33794	Sep. 29, 2021	248770
Sep. 30, 2020	38378	Oct. 30, 2021	253151
Oct. 30, 2020	52612	Nov. 30, 2021	254979
Nov. 30, 2020	83316	Dec. 30, 2021	288951
Dec. 30, 2020	96251	Jan. 30, 2022	321234
Jan. 30, 2021	100675	Feb. 28, 2022	322930
Feb. 28, 2021	105648	Mar. 30, 2022	323402
Mar. 30, 2021	132646		

and trained personnel. We therefore make the assumption that the disease spread unabated and thus the number of active cases could be higher than those declared by the ministry of health (MOH). The presence of asymptomatic persons (infected persons who do not show any symptoms of COVID-19) cannot be ruled out. The initial conditions for the state variables utilized for this study are as follows: $V_h(0) = 600$, $E_h(0) = 5500$, $I_{hA}(0) = 550$ and $R_h(0) = 60$. The total population in Kenya considered in the simulation is N(0)=54,027,487 [27], thus $S_h(0) = N(0) - V_h(0) - E_h(0) - I_{hA}(0) - I_h(0) - R_h(0)$.

The curve fit for our model is depicted in the figure (2) and its evident that our model has the best fitting to the reported data. The estimated values of parameters for real COVID-19 cases in Kenya during the period under consideration (see table (4)) produces the basic reproduction number $R_v = 1.0551339$, which is larger than the COVID-19 threshold value of one(1).

3.1. Sensitivity Analysis

Sensitivity analysis is an important tool in mathematical modeling as it aids in unearthing the extend of influence various parameters have to the disease transmission and prevalence. With the analytical expression of the model's reproduction number, R_v, its reasonable to utilize the normalized forward sensitivity index of R_v that depends differentially on a parameter $\hbar_i$, as defined by [33] and mathematically expressed as:

$$\Xi_{\hbar_i}^{R_v} = \frac{\partial R_v}{\partial \hbar_i} \times \frac{\hbar_i}{R_v},$$

where $\hbar_i$ are the various model parameters whose sensitivity on R_v is to be obtained. From table (5), it is evident that β, ω, ξ and φ have a positive effect on R_v while the rest of the parameters have a negative impact. For instance, 10% increase(decrease) in ξ causes a corresponding increase(decrease) in R_v by 0.781661% while 10% increase(decrease) in κ

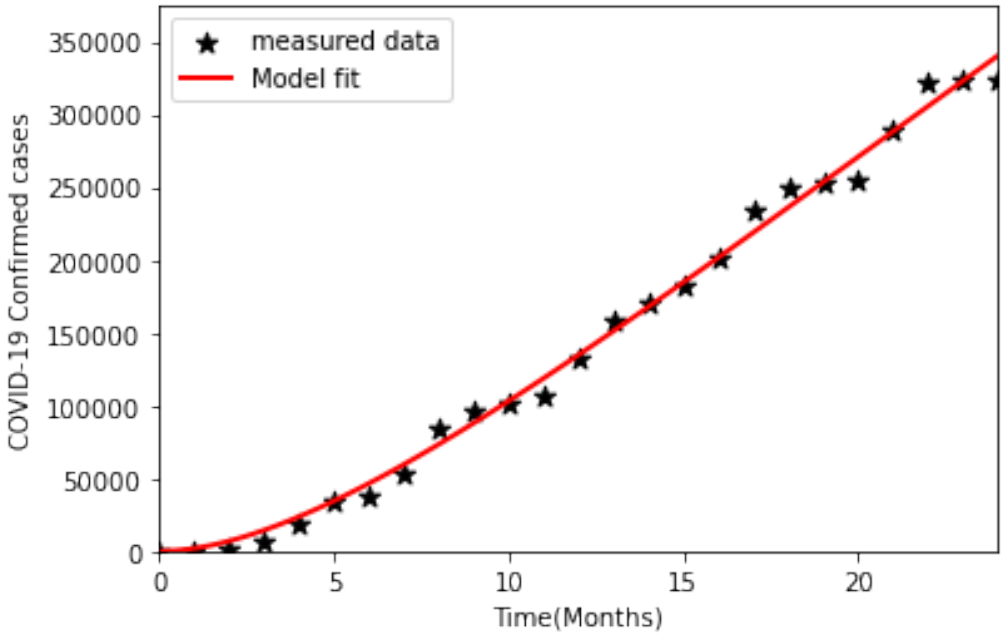

Figure 2: The reported data versus model fitting for Kenya from March 30th, 2020 to March 30th, 2022

results in a corresponding decrease(increase) in R_v by 0.904906%. It can be depicted from the table 5 that β, φ, ξ, κ and θ are the most sensitive to R_v since small perturbations to these parameters leads to a significant change in R_v.
In figure (3), panels (a) and (b) respectively show the effects of transmission coefficients β and the modification factor for asymptomatic individuals ξ to reproduction number dynamics. These parameters have a positive impact on the value of R_v in that increase(decrease) in these parameters causes a corresponding increase(decrease) in R_v. Moreover, from panels (c) and (d), we depict that vaccination rate θ is the most significant of these parameters in abasing COVID-19 transmission. It is also evident that increased identification and treatment rate κ of asymptomatic causes a substantial reduction on R_v.

4. Numerical results and discussion

In this section, we endeavor to discuss the behavior derived from the numerical simulations. The model parameters utilized are those listed in table (4). Figure (5) shows the temporal variations of different population compartments. From the projection, it is apparent that the asymptomatic population is responsible for upsurge of COVID-19 infections in Kenya. In figure (6) effect of reinfection coefficient on the recovered population at different values are shown. The projection shows that the cumulative number of individuals becoming susceptible is great for large values of τ and decreases when τ assumes low values

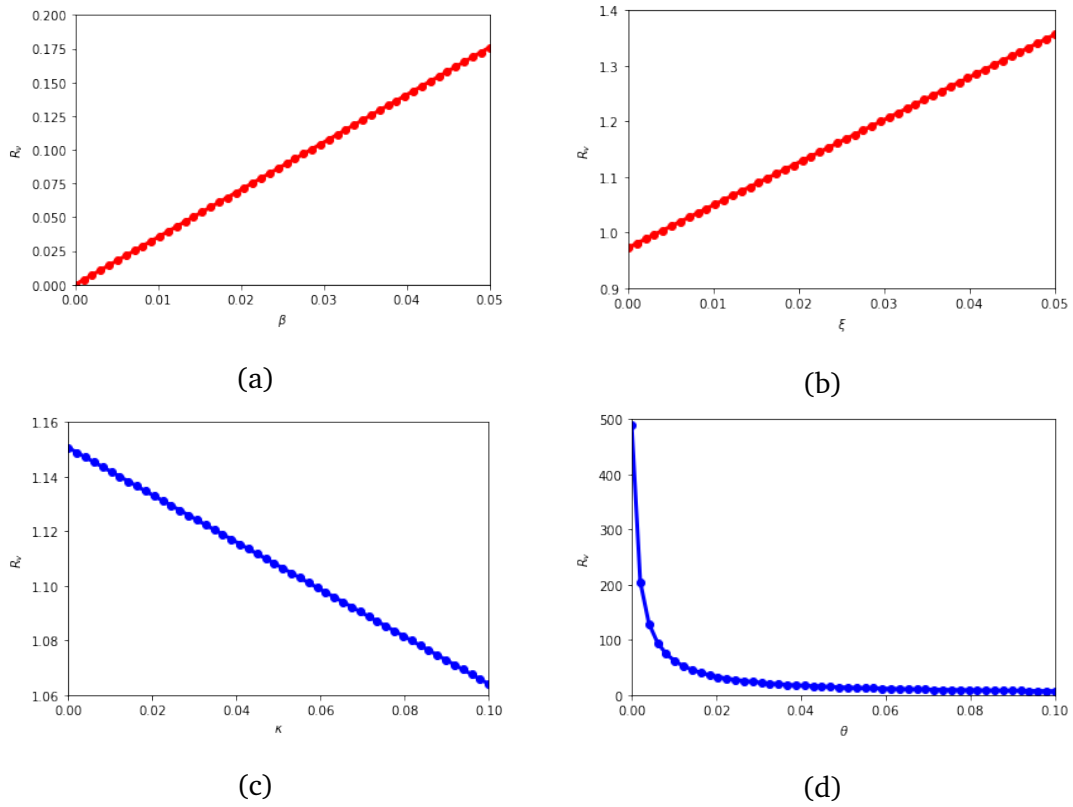

(a) (b)

(c) (d)

Figure 3: Variation of R_v with respect to: (a) the coefficient of transmission β (b) Modification factor ξ (c) the rate of detection and treatment of asymptomatic individuals κ and (d) the rate of administration of vaccine θ. The parameter values are those in table (4).

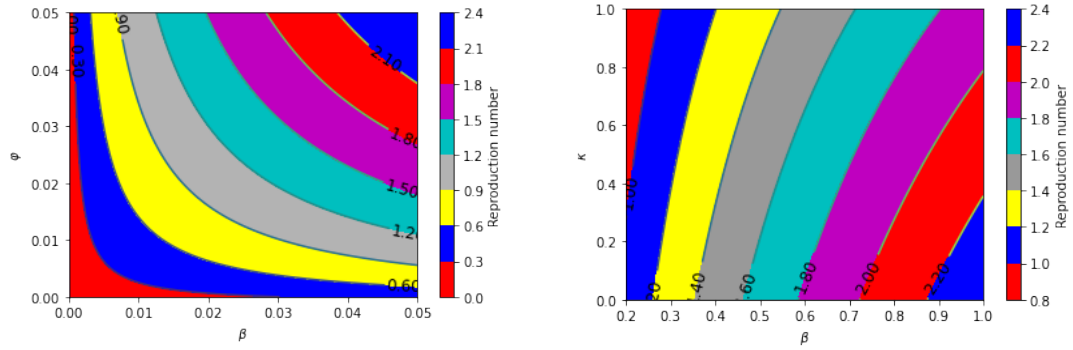

(a) (b)

Figure 4: Contour plot for R_v with respect to (a) transmission rate β and rate of waning of vaccine φ and (b) transmission rate β and rate of treatment of asymptomatic individuals κ. All parameter values are given in table (4) except for the varied parameters.

Table 4: The model parameter values and source

Parameters	Value	Source(s)
π	$\frac{1000}{67.12\times 12}$	[29, 30]
β	0.30000025	fitted
ω	$\frac{1}{7}$	[31]
μ	$\frac{1}{67.21\times 12}$	[29]
γ	0.00100	fitted
ξ	0.01075081	fitted
ϵ	0.18696757	fitted
α	1/15	[11, 34]
δ	0.58873049	fitted
κ	0.11032736	fitted
φ	0.000225	Assumed
θ	0.6785	Assumed
τ	0.00145	Assumed

Table 5: The normalized forward sensitivity indices of R_v to model parameters evaluated at the baseline parameters as displayed in the table (4).

Parameters	Sensitivity indices	Values
β	$\Xi_{\beta}^{R_v}$	+1.0000000
φ	$\Xi_{\varphi}^{R_v}$	+0.1532637
ξ	$\Xi_{\xi}^{R_v}$	+0.0781661
ω	$\Xi_{\omega}^{R_v}$	+0.0086045
ϵ	$\Xi_{\epsilon}^{R_v}$	+0.0063422
θ	$\Xi_{\theta}^{R_v}$	-0.9978456
κ	$\Xi_{\kappa}^{R_v}$	-0.0904906
α	$\Xi_{\alpha}^{R_v}$	-0.0634152
γ	$\Xi_{\gamma}^{R_v}$	-0.0015598

.

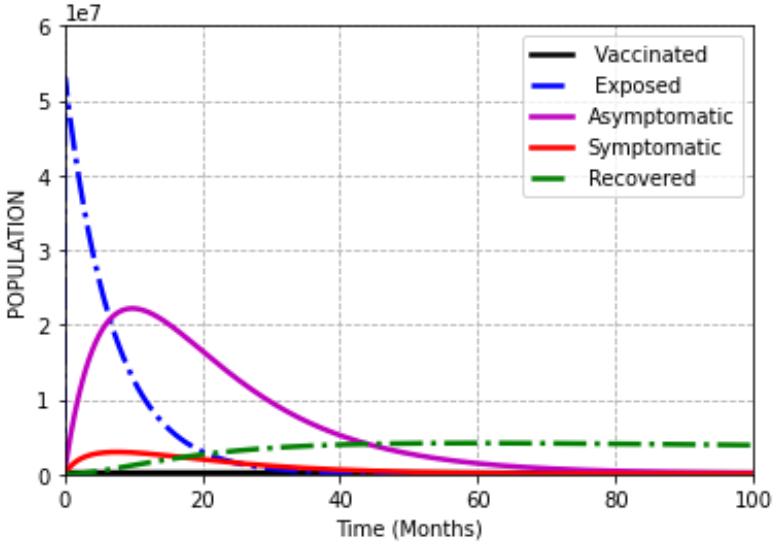

Figure 5: The time dependent variation of different population classes. All parameter values are given in table 4.

Figure (7) explores effects the variations of detection and treatment coefficient κ of asymptomatic population to the exposed, asymptomatic, symptomatic and recovered population. The projections points to the fact that increase in the value of κ leads to the decrease in the number of infectives and increase in the number of recovered individuals which ultimately leads to reduction in R_v.

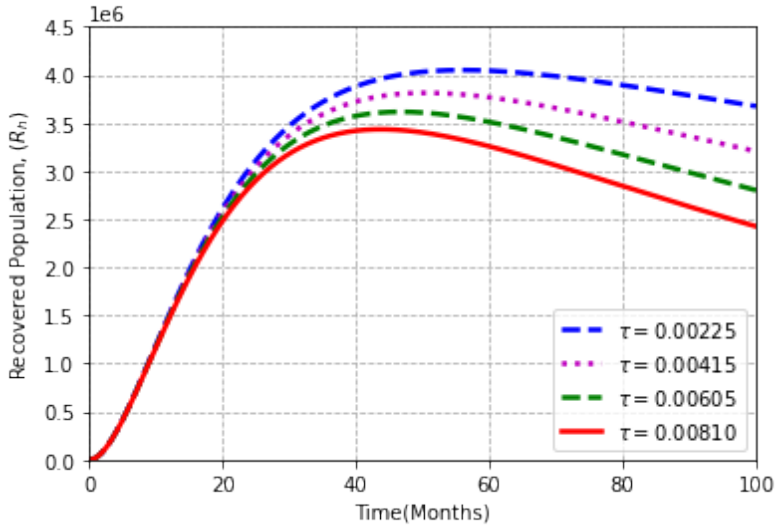

Figure 6: Effect of reinfection on the recovered individuals. All parameter values are given in table (4) except for the varied parameter and $\beta = 0.250000025$ so that $R_v = 0.8792776 < 1$.

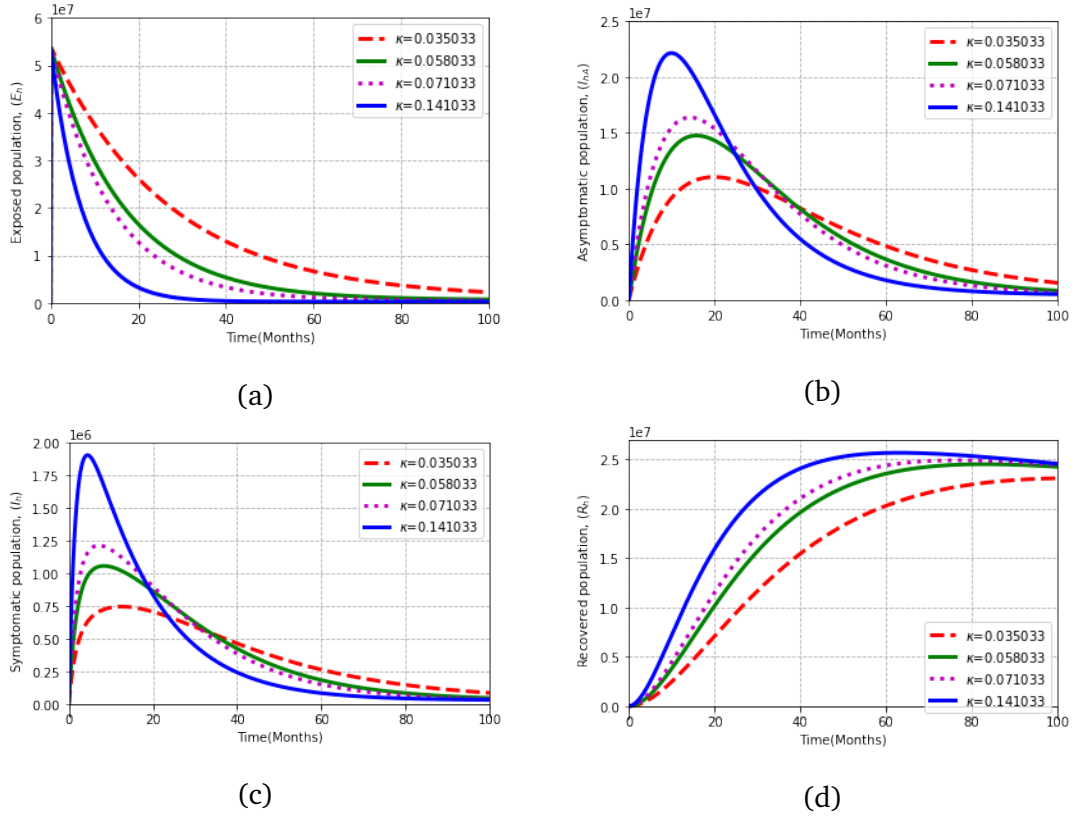

Figure 7: Projections with varying effect of detection and treatment rate of (a) exposed (b) asymptomatic (c) symptomatic and (d) recovered individuals at values of $\kappa = 0.035033(R_v = 0.933579 < 1)$, $\kappa = 0.058033(R_v = 0.916991 < 1)$, $\kappa = 0.071033(R_v = 0.907616 < 1)$, $\kappa = 0.141033(R_v = 0.857133 < 1)$. All parameter values are given in table (4) except for $\beta = 0.250000025$ and the varied parameter.

5. Discussion and conclusions

In this paper, we formulated and theoretically analyzed a non-linear deterministic model for COVID-19 by incorporating the vaccination of the susceptible and detection and treatment of the asymptomatic population as the disease transmission reduction measures. We obtained the feasible region where the model has been proved to be epidemiologically well posed. We utilized the next generation matrix method to derive the reproduction number R_v. Moreover, we verified the local stability of the disease free equilibrium point by utilizing the Jacobian matrix, trace determinant method and Routh-Hurwitz criteria.

The analytical results points to the fact that COVID-19 free-equilibrium is locally as well as globally asymptotically stable if $R_v < 1$ and unstable if $R_v > 1$. The global stability of CFE and COVID-19 endemic-equilibrium are investigated via Lyapunov function and LaSalle's Invariance principle. We also proved the condition for the existence of backward bifurcation using the center manifold theory as applied by Castillo-Chavez and Song where it was shown that this phenomenon is driven by the rate of reinfection of the recovered individuals. From epidemiological view point, the implication of this is the possible

coexistence of both CFE and CEE points even after the classical requirement of reducing the reproduction number below unit for the disease eradication has been met. This would frustrate the government and the policy makers' efforts to reduce infections.

In the segment of parameter estimation, the model is fitted with real data of COVID-19 infected cases in Kenya as reported from March 30, 2020 to March 30, 2022. In the sensitivity analysis, the normalized sensitivity indices of R_v reveals that the most sensitive parameters are β, φ and ξ with positive sign which implies that decreasing contact rate between the susceptible and the infectives through maintaining social distance, use of face masks and washing hands with soap water among other non-pharmaceutical measures would decrease R_v. Furthermore, the parameters θ and κ are the most sensitive parameters with negative sign. This signifies that to reduce COVID-19 transmission, concerted efforts towards vaccinating the susceptible, administering booster vaccine to the vaccinated individuals and early detection and treatment of the asymptomatic individuals should be prioritized by public health policy makers.

Availability of data and materials

Not applicable.

Declaration of competing interest

We as the authors declare that we have no known competing financial interests or personal relationships that could have appeared to influence the work reported in this paper.

Acknowledgement

As authors, we thank the reviewers for their useful advice, insight and comments that led to the improvement of this article and it's results.

References

[1] World Health Organization (WHO) (2020), *Coronavirus disease 2019 (COVID-19): Situation Report-78*,
[2] Abdul-rahman JM and Hugo AK (2020). *Mathematical modelling on COVID-19 transmission impacts with preventive measures: a case study of Tanzania*. Journal of Biological Dynamics. **14**(1):748-766. https://doi:10.1080/17513758.2020.1823494.
[3] Hussain T, Ozair M, Ali F, Rehman SU, Assiri TA and Mahmoud EE (2021).*Sensitivity analysis and optimal control of COVID-19 dynamics based on SEIQR model*. Results Phys.748-766. https://doi.org/10.1016/j.rinp.2021.103956
[4] Keno TD and Etana HT (2023).*Optimal Control Strategies of COVID-19 Dynamics Model*. Journal of mathematics.**2023** https://doi.org/10.1155/2023/2050684
[5] Sadek L, Sadek O, Alaoui HT, Abdo MS, Shah K and Abdeljawad T (2023).*Fractional order modeling of predicting COVID-19 with isolation and vaccination strategies in Morocco*. Computer Modeling in Engineering and Sciences.**136**(2): 1931–1950. https://DOI: 10.32604/cmes.2023.025033
[6] Ahmed I, Modu GU, Yusuf A, Kumam P and Yusuf I (2021). *A mathematical model of Coronavirus Disease (COVID-19) containing asymptomatic and symptomatic classes*. Results Phys. **21**: 103776 https://doi.10.1016/j.rinp.2020.103776
[7] Kassa SM and Njagarah JH and Terefe YA (2020). *Analysis of the mitigation strategies for COVID-19: From mathematical modelling perspective*. Chaos Solitons Fractals. **138**: 109968 https://doi:10.1016/j.chaos.2020.109968
[8] Isaacs D, Flowers D, Clarke JR, Valman HB and MacNaughton MR (1983). *Epidemiology of coronavirus respiratory infections*. Archives of disease in childhood.**58**(7):500-503. https://doi.org/10.1136/adc.58.7.500

[9] Wu L, Wang N, Chang Y, Tian X, Na D, Zhang L, Zheng L, Lan T, Wang L and Liang G (2007). *Duration of antibody responses after severe acute respiratory syndrome*. Emerging infectious diseases.**13**(10):1562–1564 https://doi.org/10.3201/eid1310.070576

[10] Alshammari FS (2020). *A Mathematical Model to Investigate the Transmission of COVID-19 in the Kingdom of Saudi Arabia*. Journal of Applied Mathematics. **2020**: 9136157. https://www.hindawi.com/journals/cmmm/2020/9136157.ris

[11] Peter OJ H.S. Panigoro HS, Abidemi A, Ojo MM and Oguntolu FA (2023). *Mathematical Model of COVID-19 Pandemic with Double Dose Vaccination*.Acta Biotheor. **2023**(71):9 https://doi.org/10.1007/s10441-023-09460-y

[12] Asha K and Nyimvu S (2020). *Onchocerciasis dynamics: modelling the effects of treatment, education and vector control*. Journal of Biological Dynamics. *14*(1):245-268. https://doi: 10.1080/17513758.2020.1745306

[13] Zenebe SK and Legesse L0 (2022). *Mathematical modeling for COVID-19 transmission dynamics: A case study in Ethiopia*. Results in physics. **34**:105191. https://doi: 10.1016/j.rinp.2022.105191

[14] Rabiu M, Willie R and Parumasur N (2020). *Mathematical analysis of a disease-resistant model with imperfect vaccine, quarantine and treatment*. Ricerche di Matematica. **69**(2): 603–627. https://doi: 10.1007/s11587-020-00496-7

[15] Asamoah J, Oduro F, Bonyah E and Seidu B (2017). *Modelling of Rabies Transmission Dynamics Using Optimal Control Analysis*. Journal of Applied Mathematics. **2017**:2451237:1-23. https://doi.org/10.1155/2017/2451237

[16] Ega TT, Luboobi LS and Kuznetsov D (2015). *Modeling the Dynamics of Rabies Transmission with Vaccination and Stability Analysis*. Emerging infectious diseases. **13**(10):409-419 https://doi: 10.11648/j.acm.20150406.13

[17] Diekmann O and Heesterbeek H (2013). "Mathematical Tools for Understanding Infectious Disease Dynamics". Princeton University Press.

[18] Yusuf TT and Benyah F (2012). *Optimal Control of Vaccination and Treatment for an SIR Epidemiological Model*. World Journal of Modelling and Simulation. **8**(3):194-204.

[19] Murray RM and Stastry SS (1994). "A Mathematical Introduction to Robotic Manipulation". Press, London.

[20] Castillo-Chavez C. and Song B (2004). *Dynamical models of tuberculosis and their applications*. Mathematical biosciences and engineering : MBE **1**(2): 361–404. https://doi: 10.3934/mbe.2004.1.361

[21] Guckenheimer J and Holmes P (1983). "Nonlinear Oscillations, Dynamical Systems and Bifurcations of Vector Fields". Springer-Verlag, New York.

[22] Nainggolan J and M. F. Ansori MF (2022). *Stability and Sensitivity Analysis of the COVID-19 Spread with Comorbid Diseases*, Symmetry. **14**(11):2269 https://doi.org/10.3390/sym14112269

[23] Nyaberi HO and Wakwabubi VW (2020). *Mathematical Modeling of the Dynamics of Infectious Diseases with Relapse*. Asian Journals of Mathematics and Computer Research. **27**(1):28-37. https://ikprress.org/index.php/AJOMCOR/article/view/4996

[24] Safi MA and Gumel AB (2011). *Mathematical Analysis of a Disease Transmission Model with Quarantine, Isolation and an Imperfect Vaccine*. Computers and Mathematics with Applications. **61**(1):3044-3070. https://doi.org/10.1016/j.camwa.2011.03.095

[25] Hale JK (1981). "Ordinary Differential Equations". Robert E. Krieger Publishing Company, Inc, New York.

[26] Worldometer (2022), *Coronavirus Pandemic in Kenya*. https:www.worldometers.info/coronavirus/country/Kenya

[27] Worldometer (2022). *Kenya Population.Available online; Assessed on (12th December 2022)*. https.//www.worldometers,info//world-population/Kenya-population

[28] Agusto FB (2013). *Optimal isolation control strategies and cost-effectiveness analysis of a two-strain avian influenza model*. Bio Systems. **113**(3): 155 –164. https://doi.org/10.1016/j.biosystems.2013.06.004

[29] Bruno B (2013). *Analysis of a malaria model with mosquito host choice and bed-net control*. International Journal of Biomathematics. **8**(6). https://DOI:10.1142/S1793524515500771

[30] Tchoumi SY and Rwezaura H. and Tchuenche J M (2022). *Dynamic of a two-strain COVID-19 model with vaccination*. Results in physics. **39**: 105777. https://doi: 10.1016/j.rinp.2022.105777

[31] Bugalia S, Bajiya VP, Tripathi JP, Li MT and Sun GQ (2022). *Mathematical modeling of COVID-19 transmission: the roles of intervention strategies and lockdown*. Mathematical biosciences and engineering : MBE. **17**(5): 5961–5986. https://doi.org/10.3934/mbe.2020318

[32] Newville M, Stensitzki T, Allen D and Ingargiola A (2014). *LMFIT: Non-Linear Least-Square Minimization and Curve-Fitting for Python*. https://doi.org/10.5281/zenodo.11813

[33] Chitnis N, Hyman J and Cushing J (2008). *Determining Important Parameters in the Spread of Malaria Through the Sensitivity Analysis of a Mathematical Model*. Bulletin of mathematical biology. **70**(5):1272-1296. https://doi: 10.1007/s11538-008-9299-0

[34] Okuonghae D and Omame A (2020). *Analysis of a mathematical model for COVID-19 population dynamics in Lagos, Nigeria*. Chaos, solitons, and fractals. **139**:110032. https://doi: 10.1016/j.chaos.2020.110032